Bioorganic & Medicinal Chemistry Letters 25 (2015) 2668–2674

Contents lists available at ScienceDirect

Bioorganic & Medicinal Chemistry Letters

journal homepage: www.elsevier.com/locate/bmcl

Design, synthesis and pharmacology of 1,1-bistrifluoromethylcarbinol derivatives as liver X receptor β-selective agonists

Minoru Koura, Takayuki Matsuda, Ayumu Okuda, Yuichiro Watanabe, Yuki Yamaguchi, Sayaka Kurobuchi, Yuuki Matsumoto, Kimiyuki Shibuya *

Tokyo New Drug Research Laboratories, Pharmaceutical Division, Kowa Co., Ltd, 2-17-43, Noguchicho, Higashimurayama, Tokyo 189-0022, Japan

ARTICLE INFO

Article history:
Received 17 December 2014
Revised 3 April 2015
Accepted 23 April 2015
Available online 5 May 2015

Keywords:
Liver X receptor (LXR) β-selective
LDL-C
1,1-Bistrifluoromethylcarbinol
Anti-atherosclerosis

ABSTRACT

A novel series of 1,3-bistrifluoromethylcarbinol derivatives that act as liver X receptor (LXR) β-selective agonists was discovered. Structure–activity relationship studies led to the identification of molecule **62**, which was more effective (E_{max}) and selective toward LXRβ than T0901317 and GW3965. Furthermore, **62** decreased LDL-C without elevating the plasma TG level and significantly suppressed the lipid-accumulation area in the aortic arch in a Bio F_1B hamster fed a diet high in fat and cholesterol. We demonstrated that our LXRβ agonist would be potentially useful as a hypolipidemic and anti-atherosclerotic agent. In this manuscript, we report the design, synthesis and pharmacology of 1,3-bistrifluoromethylcarbinol derivatives.

In our drug discovery program dedicated toward the development of novel anti-atherosclerotic agents, we have focused our continuing efforts on LXR agonists that offer the possibility of reverse cholesterol transport (RCT) from atherosclerotic lesions. LXRs are ligand-activated transcription factors involved in cholesterol metabolism, glucose homeostasis, inflammation and lipogenesis.[1] LXRα (known as NR1H3) is the dominant subtype in the liver, small intestine, and macrophages, whereas LXRβ (known as NR1H2) is distributed ubiquitously. LXR activation is known to regulate the ATP-binding cassette transporter A1 (ABCA1), ABCG1 and ABCG5/G8 expression and cholesterol metabolism to increase the high-density lipoprotein cholesterol (HDL-C) levels and to serve in cholesterol efflux and excretion.[2]

Several studies have reported that T0901317 and GW3965 exhibit the potentially useful property of increasing the plasma HDL-C and decreasing atherosclerotic lesions in mouse models of atherosclerosis (Fig. 1).[3,4] However, elevations in the plasma and hepatic triglyceride (TG) levels were observed as significant side effects.[5] This lipogenesis originates from the expression of sterol regulatory element-binding protein-1c (SREBP-1c), which is induced by LXRα activation. To suppress this undesirable effect in the LXR agonist, we made efforts to differentiate between these two LXR subtypes and discovered that the 2-oxochromene derivative **3** can act as a LXRβ-selective agonist. Derivative **3** also increased the HDL-C levels without a significant TG elevation and resulted in a decrease in the lipid-accumulation areas in the aortic arch in a Bio F_1B hamster fed a diet high in fat and cholesterol.[6]

However, further developments and investigations on the potency and selectivity toward LXRβ and improvements in the physical properties and pharmacokinetics are required. In this manuscript, we report the modification of the structure of the head moiety in our molecular design (head-to-tail) and identify **62** as the optimized molecule. For this purpose, we focused on the His435-Trp457 activation switch[7] to enhance the interaction between the ligand and the LXRβ receptor. First, we speculated that the trifluoromethyl group may be a key factor in the head structure for LXR activation, as shown in Figures 1 and 2. Second, we aimed to modify the head structure of **3**[6] and transformed its structure into the following four types of compounds (**4**, **5**, **6** and **7**)[8,9]: (1) the removal of the carbonyl group at the 2-position of the chromene moiety and the reduction of the double bond gave the chromane structure **4**, (2) the contraction of the six-membered ring in **4** and the incorporation of an additional trifluoromethyl group yielded the 1,3-dihydroisobenzofuran structure **5**, (3) the cleavage of the C–O bond in the five-membered ring of **5** gave the carbinol structure **6**, and (4) the incorporation of a *n*-propyl group on the benzene ring yielded the bis-*n*-propyl phenyl structure **7** (Fig. 3).

The head of **4**, which was the requisite 8-*n*-propyl-4-(trifluoromethyl)chroman-7-ol (**11**), was prepared from 7-hydroxy-8-*n*-propyl-4-(trifluoromethyl)-2*H*-chromen-2-one (**8**) through a three-step protocol, as depicted in Scheme 1. The reduction of **8**

* Corresponding author. Tel.: +81 42 391 6211; fax: +81 42 395 0312.
E-mail address: k-sibuya@kowa.co.jp (K. Shibuya).

http://dx.doi.org/10.1016/j.bmcl.2015.04.080
0960-894X/

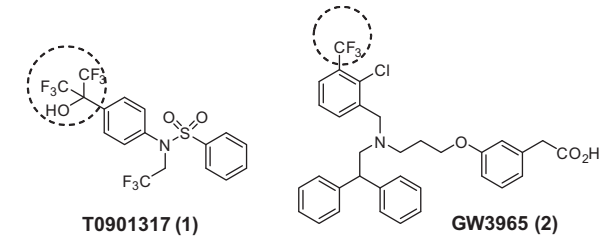

Figure 1. Structures of LXR agonists from Tularik and GlaxoSmithKline.

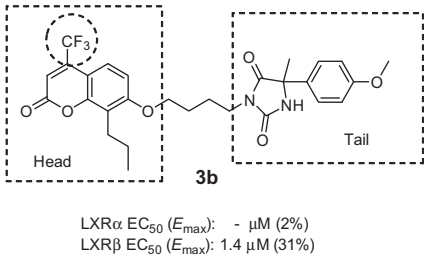

Figure 2. Head-to-tail design of our discovered LXRβ-selective agonist.

with $LiAlH_4$ afforded the alcohol **9**, which was subsequently brominated using a combination of triphenylphosphine and carbon tetrabromide to give the bromide **10**. The cyclization of **10** under basic conditions provided the desired chroman **11**.

The head of **5**, the requisite 4-*n*-propyl-1,1-bis-(trifluoromethyl)-1,3-dihydroisobenzofuran-5-ol (**23**), was prepared from methyl 3-hydroxybenzoate (**12**) through 12 steps, as depicted in Scheme 2. Methyl 3-allyloxybenzoate (**13**) was obtained by the allylation of **12** with allyl chloride in the presence of a base. A thermal Claisen rearrangement of **13** gave a mixture of methyl 2-allyl-3-hydroxybenzoate (**14a**) and methyl 4-allyl-3-hydroxybenzoate (**14b**), and this reaction was followed by hydrogenation with Pd/C in MeOH under a hydrogen atmosphere to provide a mixture of methyl 2-*n*-propyl-3-hydroxybenzoate (**15a**) and methyl 4-*n*-propyl-3-hydroxybenzoate (**15b**). The reduction of **15a** with $LiAlH_4$ afforded 3-hydroxymethyl-2-*n*-propylphenol (**16**), which was subsequently halogenated using tetrabutylammonium tribromide to give the bromobenzene **17**. To distinguish the two hydroxyl groups in **17**, we first protected the primary alcohol with 3,4-dihydro-*2H*-pyran (DHP) in the presence of *p*-TsOH and then protected the phenol of **18** with chloromethyl methyl ether (MOMCl) in the presence of NaH to produce the bis-protected bromobenzene **19**. The lithiation of **19** with *n*-BuLi was followed by reaction with 1,1,1,3,3,3-hexafluoroacetone to give the carbinol **20**. After the deprotection of THP, the cyclization of the resulting two hydroxyl groups
in **21** was performed through the Mitsunobu reaction[10] to form the 1,3-dihydroisobenzofuran intermediate **22**. The cleavage of the MOM ether in **22** under acidic conditions furnished the desired phenol **23**.

The head of **6**, the requisite 4-(1,1,1,3,3,3-hexafluoro-2-(hydroxy)propan-2-yl)-2-*n*-propylphenol (**28**), was prepared from methyl 4-hydroxybenzoate (**24**) through a nine-step procedure, as depicted in Scheme 3. Methyl 3-*n*-propyl-4-hydroxybenzoate (**25**) was obtained through the following steps: (i) the allylation of **24** with allyl chloride, (ii) a thermal Claisen rearrangement of phenoxy allyl ether, and (iii) the conversion of the allyl group into an *n*-propyl group via hydrogenation. The benzylation of phenol **25** followed by the hydrolysis of the methyl benzoate gave the benzoic acid **26**. The acid chloride was obtained through the reaction of **26** with thionyl chloride, which was then bis-trifluoromethylated using CF_3TMS in the presence of tetramethylammonium fluoride to provide the 1,1-bistrifluoromethylcarbinol **27**. After the protection of the carbinol with MOMCl, the benzyl ether was deprotected via hydrogenolysis to yield **28**.

The head of **7**, the requisite, 4-(1,1,1,3,3,3-hexafluoro-2-(methoxymethoxy)propan-2-yl)-2,6-di-*n*-propylphenol (**32**), was prepared through a procedure similar to that described above.

Alkyl phenyl ketone **34** was obtained by a Friedel–Crafts acylation[11] of **33** with an alkylacid anhydride. Imidazolidine-2,4-dione **35** was prepared via a Bucherer–Bergs reaction[12] of ketone **34** using NaCN and $(NH_4)_2CO_3$, as depicted in Scheme 4.

A series of 1,1-bistrifluoromethylcarbinol derivatives including **37** and **39** was prepared as depicted in Scheme 5. The alkylation

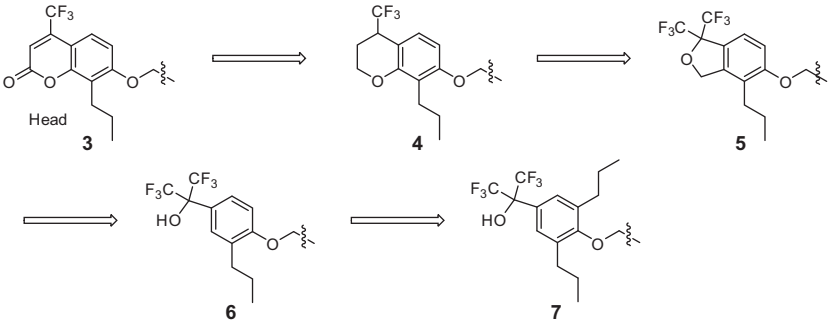

Figure 3. Molecular design to modify the head structure of **3**.

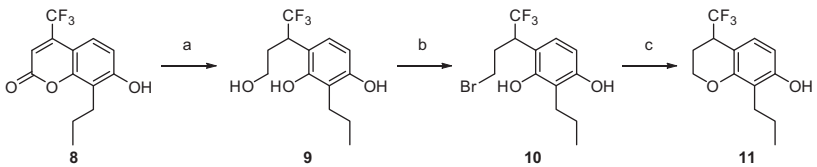

Scheme 1. Reagents and conditions: (a) $LiAlH_4$, THF, 0 °C, 1 h; (b) PPh_3, CBr_4, THF, rt, 10 min; (c) K_2CO_3, DMF, rt, overnight, 70% yield after the three steps.

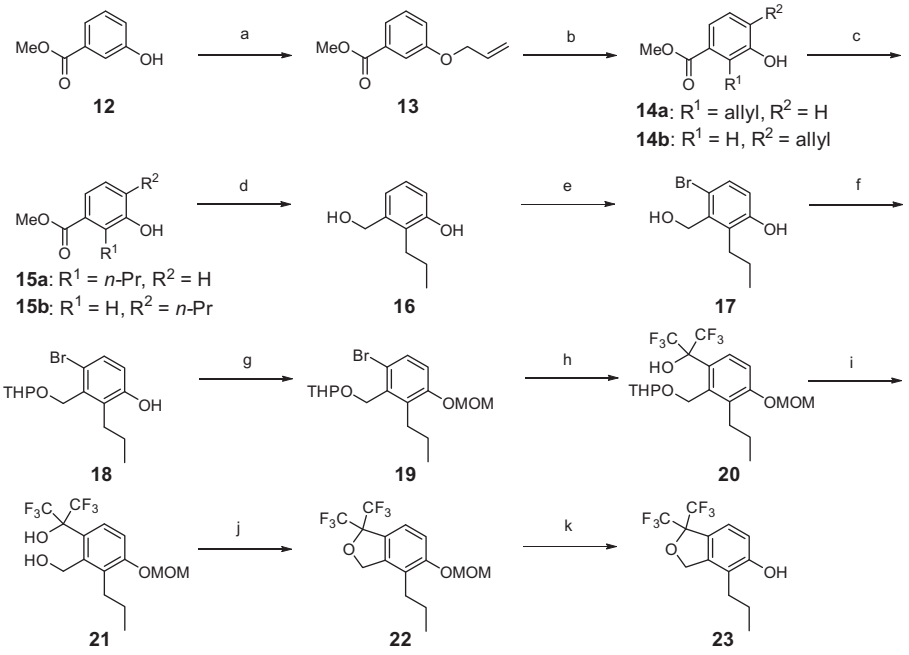

Scheme 2. Reagents and conditions: (a) allyl chloride, K_2CO_3, DMF, 100 °C, overnight, 95%; (b) $PhNMe_2$, 210 °C, 19 h, 80%; (c) H_2, Pd/C, MeOH, rt, 2 h, 56%; (d) $LiAlH_4$, THF, rt, 2.5 h, 91%; (e) *n*-Bu_4NBr_3, CH_2Cl_2/MeOH, rt, 1 h, 67%; (f) DHP, *p*-TsOH-H_2O, CH_2Cl_2, rt, 2 h, 78%; (g) MOMCl, NaH, DMF, 0 °C to rt, overnight, 83%; (h) (i) *n*-BuLi, THF, −78 °C, 30 min and then −40 °C, 1.5 h; (ii) CF_3COCF_3, THF, −78 °C, 10 min then 0 °C, 3 h, 65%; (i) aq AcOH, THF, rt, 2 h, 90%; (j) DEAD, PPh_3, CH_2Cl_2, rt, 2 h, 93%; (k) aq HCl, MeOH, rt, 2 h, 96%.

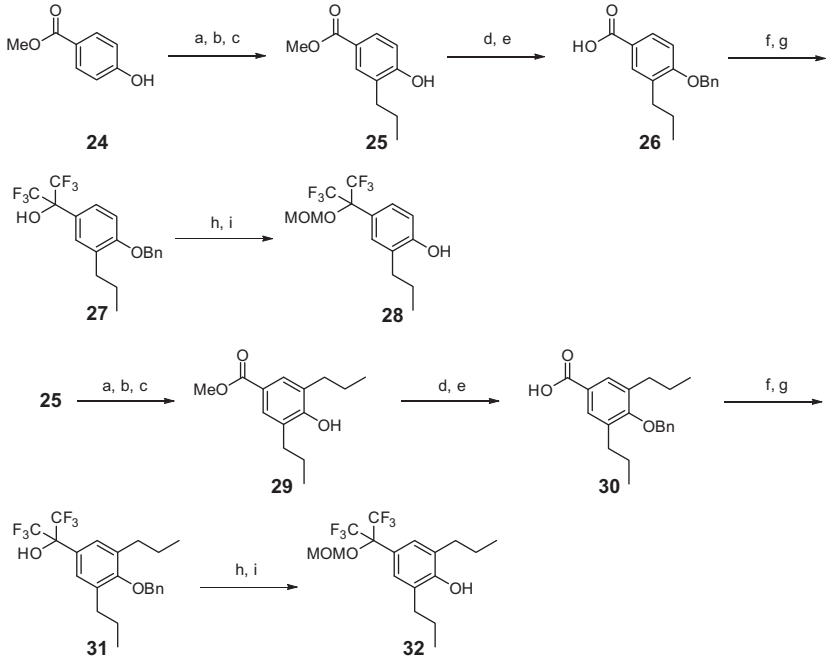

Scheme 3. Reagents and conditions: (a) allyl chloride, K_2CO_3, DMF, 50 °C, overnight, 99%; (b) $PhNMe_2$, 210 °C, 12 h, 60%; (c) H_2, Pd/C, MeOH, rt, 2 h, 99%; (d) BnBr, K_2CO_3, DMF, 80 °C, 2 h, 99%; (e) 2N NaOH aq, EtOH, 50 °C, 2 h, 98%; (f) $SOCl_2$, reflux, 1 h; (g) CF_3TMS, Me_4NF, DME, −78 °C to rt, 67–72% after these two steps; (h) MOMCl, NaH, THF, rt, overnight, 89–99%; (i) H_2, Pd/C, MeOH, rt, 2 h, 85–99%.

of **28** and **32** with 1,4-dibromobutane and their subsequent reaction with imidazolidine-2,4-dione **35** gave **36** and **38**, respectively. The MOM ethers of **36** and **38** were then cleaved under acidic conditions to afford **37** and **39**, respectively.

To investigate what type of head structure is favorable, we evaluated the activities of the four newly designed derivatives (**4**, **5**, **6** and **7**) in combination with two types of tail structure (a, b) through GAL4-LXRαβ luciferase assays. We defined two types of tail

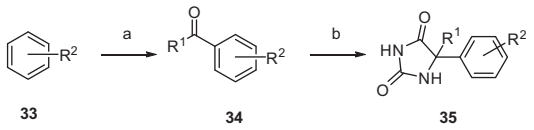

Scheme 4. Reagents and conditions: (a) $(R^1CO)_2O$, $AlCl_3$, DMC, rt, 90%; (b) NaCN, $(NH_4)_2CO_3$, EtOH (aq), 70 °C, 85%.

structure for the following reasons: (1) 1-*N*-methyl-5,5-dimethyl-imidazolidine-2,4-dione (tail a) was the basic structure used for diversity and (2) 5-(4-methoxyphenyl)-5-methyl-imidazolidine-2,4-dione (tail b) was the satisfactory structure in **3b**.[13] The results were summarized and are shown in Table 1.

The chroman moiety **4a** markedly decreased the potency (EC_{50}) and efficacy (E_{max}) toward LXRβ compared with **3a**, whereas the dihydroisobenzofuran moiety **5a** and **5b** increased the EC_{50} and E_{max} values toward LXRβ compared with **3a** and **3b**, respectively. To our delight, the 1,1-bistrifluoromethylcarbinol moieties **6a**, **7a** and **7b** significantly enhanced the E_{max} values toward both LXRs.[14] Therefore, we decided to subject the moieties 6 and 7 as promising core structures in the head-to-tail design to further development. Although 'tail a' was superior to 'tail b' in terms of the EC_{50} and E_{max} values, further improvement in the selectivity (EC_{50} LXRα/EC_{50} LXRβ) was limited. We then focused on the substitutable 'tail b' and investigated which substituents at R^1 and R^2 were more favorable on the imidazoline-2,4-dione moiety. To improve the EC_{50} and E_{max} values and the selectivity of the optimized combinations, we evaluated a series of mono-*n*-propyl 1,1-bistrifluoromethyl-carbinol (**37**) and bis-*n*-propyl 1,1-bistrifluoromethylcarbinol (**39**) compounds composed of 'tail b' with a linker through GAL4-LXRα/β luciferase assays. The results are summarized in Table 2.

In a series of mono-*n*-propyl type compounds **37** (**6b**, **40**–**60**), in the cases in which R^1 was a methyl group and R^2 was a variety of substituents on the benzene in 5-phenyimidazolidine-2,4-dione (**40**–**56**), the 3,4-methylendioxyphenyl group in **49** and 2,3-dihydrobenzo[*b*][1,4]dioxin-6-yl group in **50** showed greater EC_{50} values for LXRβ compared with **6b**. The 4-phenyl group in **54** exhibited a greater E_{max} value toward LXRβ. In contrast, the 4-dimethylaminophenyl group in **51**, the 4-chlorophenyl group in **52**, the 3,4-dichlorophenyl group in **53**, the 4-trifluoromethylphenyl group in **55** and the 4-nitorophenyl group in **56** decreased the E_{max} values for LXRβ compared with **6b**. In addition, if R^1 was an ethyl or *n*-propyl group instead of a methyl group, the EC_{50} and E_{max} values toward LXRβ were increased (**57**, **58**, **59**, **60**) compared with **6b**. In a series of bis-*n*-propyl type compounds **39** (**7b**, **61**–**69**), the 4-ethoxyphenyl group in **61** and the 4-isopropylphenyl group in **62** showed desirable E_{max} values for LXRβ and selectivities (E_{max} for LXRβ/E_{max} for LXRα).

Table 1
LXR activities of the newly designed head structure[a]

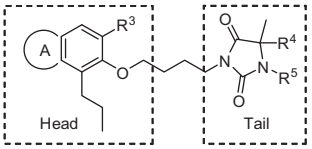

R^3 = H or *n*-propyl
a: R^4 = R^5 = Me
b: R^4 = 4-methoxyphenyl, R^5 = H

Compound	Head structure	Tail	LXRa EC_{50}[b] (%)[c]	LXRb EC_{50}[b] (%)[c]
3	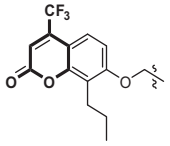	a	2.4 (7)	1.0 (51)
		b	ia (2)	1.4 (31)
4	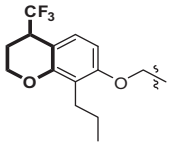	a	nd (3)	2.2 (21)
		b	—	—
5	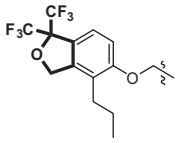	a	2.2 (82)	0.86 (95)
		b	1.7 (81)	1.0 (104)
6	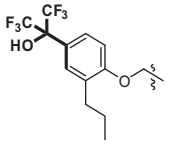	a	3.2 (97)	1.9 (162)
		b	2.8 (12)	1.8 (32)
7	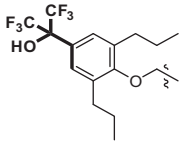	a	0.71 (107)	0.56 (142)
		b	1.6 (51)	1.4 (66)

nd = not determined.
ia = inactive at 10 μM.
[a] The GAL4-LXR luciferase assay was performed with a maximal dose of 30 μM. The results are given as the means from two independent experiments.
[b] The EC_{50} data are reported in μM.
[c] The E_{max} is defined as the percentage ratio of the maximum fold induction for the test compound to the fold induction for T0901317 at 10 μM in the same experiment.[13]

Based on the results presented in Table 2, we selected **49**, **57** and **62** for further evaluation because their profiles showed lower E_{max} values for LXRα and higher E_{max} values for LXRβ. These compounds outperformed our previously discovered LXRβ agonist **3b** in terms

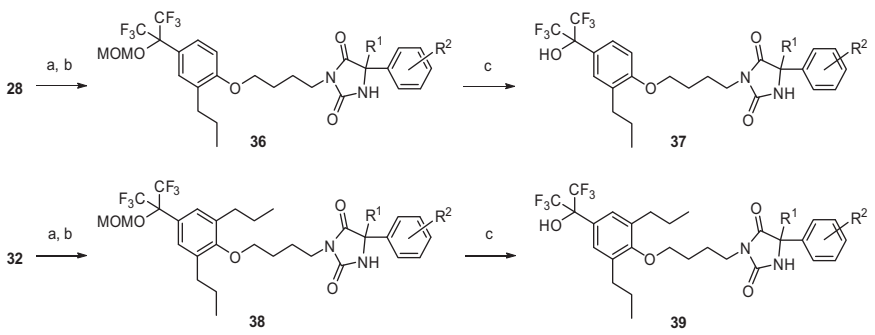

Scheme 5. Reagents and conditions: (a) 1,4-dibromobutane, K_2CO_3, DMF, rt, 71–94%; (b) **35**, K_2CO_3, DMF, rt, 99%; (c) HCl/EtOAc, rt, 81–82%.

Table 2
LXR activities of mono-*n*-propyl **37** and bis-*n*-propyl **39** in the 1,1-bistrifluoromethylcarbinol derivatives[a]

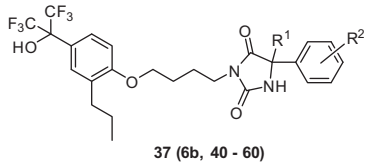

37 (6b, 40 - 60)

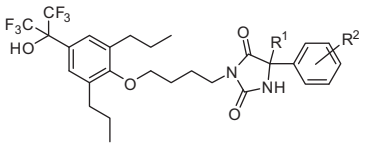

39 (7b, 61-69)

Compound	R^1	R^2	LXRα EC_{50}[b] (%)[c]	LXRβ EC_{50}[b] (%)[c]
6b	Me	4-OMe	2.8 (12)	1.8 (32)
40	Me	H	2.0 (42)	12 (15)
41	Me	4-Me	2.2 (37)	2.0 (23)
42	Me	4-*i*-Pr	1.9 (8)	2.2 (64)
43	Me	2-OMe	2.7 (7)	ia (0)
44	Me	3-OMe	2.4 (15)	2.2 (70)
45	Me	3,4-diOMe	2.4 (13)	1.3 (65)
46	Me	4-OEt	1.3 (89)	1.1 (53)
47	Me	4-O-*i*-Pr	1.8 (67)	2.8 (51)
48	Me	4-OCF_3	2.8 (33)	1.2 (125)
49	Me	3,4-OCH_2O	1.7 (54)	0.5 (118)
50	Me	3,4-$O(CH_2)_2O$	1.2 (71)	0.4 (171)
51	Me	4-$N(Me)_2$	2.2 (8)	2.7 (27)
52	Me	4-Cl	2.2 (23)	1.8 (29)
53	Me	3,4-diCl	1.7 (4)	1.1 (43)
54	Me	4-Ph	1.4 (108)	1.0 (174)
55	Me	4-CF_3	2.5 (10)	1.8 (25)
56	Me	4-NO_2	2.2 (51)	1.9 (39)
57	Et	4-OMe	2.3 (48)	1.0 (150)
58	Et	3,4-OCH_2O	1.5 (72)	0.7 (172)
59	*n*-Pr	3,4-OCH_2O	2.3 (42)	1.3 (72)
60	Et	3,4-$O(CH_2)_2O$	1.5 (88)	0.7 (172)
7b	Me	4-OMe	1.6 (51)	1.4 (66)
61	Me	4-OEt	0.9 (43)	0.8 (148)
62	Me	4-O-*i*-Pr	1.1 (26)	1.2 (146)
63	Me	4-OCF_3	1.8 (62)	2.7 (61)
64	Me	3,4-OCH_2O	0.4 (89)	0.1 (101)
65	Me	3,4-$O(CH_2)_2O$	0.5 (94)	0.6 (70)
66	Me	4-*i*-Pr	1.8 (21)	1.7 (25)
67	Me	4-Ph	1.2 (31)	1.6 (58)
68	Et	4-OMe	1.2 (85)	1.1 (81)
69	Et	3,4-OCH_2O	0.6 (118)	0.7 (118)

ia = inactive at 10 μM.
[a] The GAL4-LXR luciferase assay was performed with a maximal dose of 30 μM. The results are given as the means from two independent experiments.
[b] The EC_{50} data are reported in μM.
[c] The E_{max} is defined as the percentage ratio of the maximum fold induction for the test compound to the fold induction for T0901317 at 10 μM in the same experiment.[13]

of the dose-response curves of LXRα and LXRβ activities, as shown in Figure 4.

To discriminate between the pharmacokinetic properties of these agonists, we conducted an in vitro test of liver clearance (CL) in mice, hamsters and humans. The metabolic stability of the 1,1-bistrifluoromethylcarbinol derivative **62** was greatly improved and superior to those of **3b**, **49** and **57**, as shown in Table 3.

We selected **62**, which displayed a relatively weak activity for LXRα and a higher activity for LXRβ and metabolic resistance, and then conducted an in vivo test of **62** in a Bio F_1B hamster fed a diet high in fat and cholesterol (Table 4). The Bio F_1B hamster was more responsive to diet-induced atherosclerosis than mice and an adequate atherosclerosis model used for the evaluation of lipid-modulating agents.[15] T0901317, at a dose of 10 mg/kg, significantly decreased the area of lipid accumulation in the aortic arch (40% relative to the control) but significantly elevated the plasma TG level (251%) and TC level (124%) despite decreasing both the HDL-C (76%) and LDL-C (75%) levels.[16] The oral administration of **62** at a dose of 100 mg/kg considerably decreased the area of lipid accumulation, which was accompanied with a reduction in the LDL-C (45%) and a slight elevation in the plasma TG level. Additionally, **62** significantly decreased the TC level (53%), whereas T0901317 increased it.

Based on these results, the suppression of lipid accumulation by **62** could be attributed to the marked reduction of the LDL-C level under the conditions of a diet high in fat and cholesterol. In contrast, these findings suggested that the significant reduction of HDL-C could not substantially serve the RCT from atherosclerotic lesions. The obtained pharmacological effectiveness should not be identified as a direct anti-atherosclerotic effect but rather a hypolipidemic one. Accordingly, we monitored the plasma drug concentration of **62** and its major metabolite **70** after the oral administration of **62** at a dose of 100 mg/kg, as shown in Figure 5.[17] Compound **62** was oxidatively metabolized to afford the carboxylic acid **70** and then disappeared. The C_{max} of **62** was 406 ng/mL (0.6 μM) and did not reach the EC_{50} level (1.2 μM) associated with LXRβ agonistic action.

This result was insufficient to upregulate ABCA1 in the peripheral blood, resulting in a decrease in the HDL-C level. In contrast, the long exposure time (6–8 h) to **62** in the intestine was sufficient

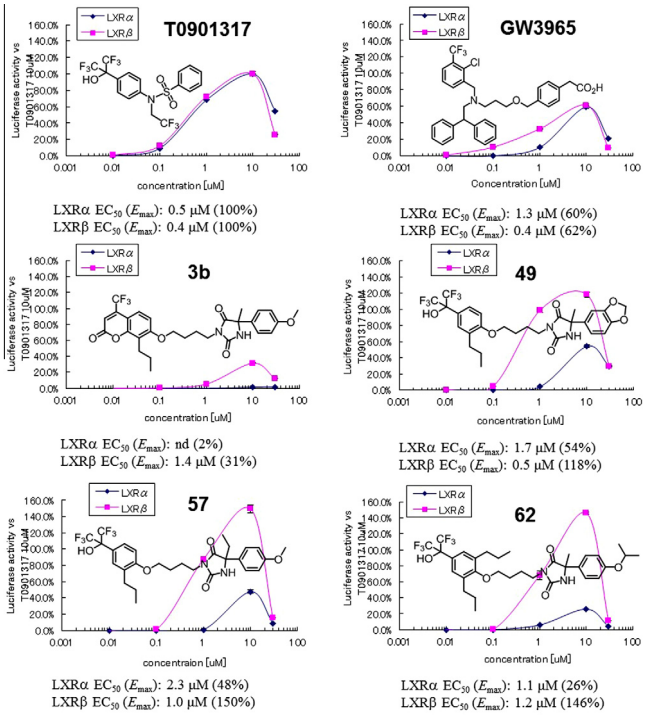

Figure 4. Dose–response curves of T0901317, GW3965, **3b**, **49**, **57** and **62**.

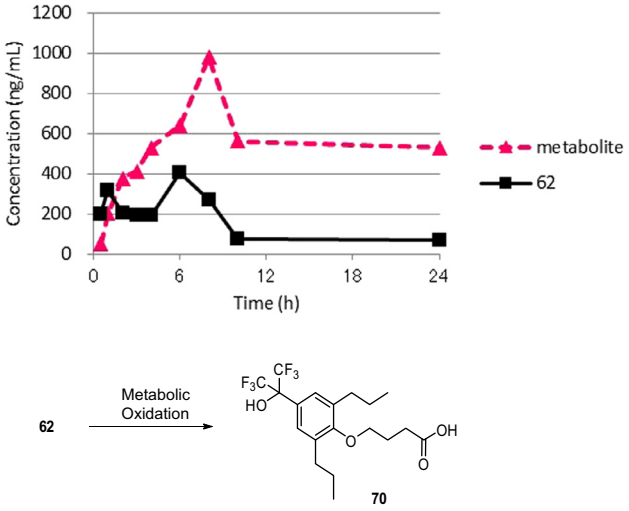

Figure 5. Drug concentrations of **62** and metabolite **70**.[17]

Table 3
CL (μL/min/mg protein) of each animal obtained through an in vitro assay*

Compound	Mouse	Hamster	Human
3b	397	500	393
49	73	351	31
57	65	295	73
62	44	49	42

* The CL values of compounds **3b**, **49**, **57**, **62** were assessed using hepatic microsomes from each animal (mouse, hamster and human).

Table 4
In vivo study with T0901317 and **62**[14]

Compound	Dose (mg/kg)	TC (%)	HDL-C (%)	LDL-C (%)	Plasma TG (%)	Area of lipid accumulation (%)
T0901317	10	124*	76*	75*	251*	40*
62	10	87	98	94	97	86
	30	96	92	91	145*	84
	100	53*	75*	45*	112	49*

* $p<0.05$; statistical analysis was conducted using Dunnett's test. The % value was calculated relative to the control.

to inhibit the absorption of cholesterol from the intestine by the upregulation of ABCA1,[18] and this compound plays a substantial role in inhibiting cholesterol absorption. Therefore, we discovered the potential utility of the hypolipidemic agent.

In conclusion, the 1,1-bistrifluoromethylcarbinol moiety (head) played an important role as a potent and selective LXRβ agonist. The novel LXRβ agonist **62** decreased TC without a significant TG elevation and resulted in a decrease in the lipid-accumulation area in the aortic arch in a Bio F_1B hamster fed a diet high in fat and cholesterol. However, issues remain with **62**, including the potency, selectivity and PK profiles. An even more favorable modulator profile than that of **62** is required for human therapeutic use. Further development is underway.

Acknowledgments

We thank Dr. S. Tanabe, Director of Tokyo New Drug Research Laboratories, Kowa Co., Ltd, for his support.

Supplementary data

Supplementary data (pharmacological experimental details, pharmacokinetic experimental details, general preparation procedure and analytical data of all of the synthetic compounds) associated with this article can be found, in the online version, at http://dx.doi.org/10.1016/j.bmcl.2015.04.080.

References and notes

1. (a) Nuclear Receptors Nomenclature Committee *Cell* **1999**, *97*, 161; (b) Willy, P. J.; Umesono, K.; Ong, E. S.; Evans, R. M.; Heyman, R. A.; Mangelsdorf, D. J. *Genes Dev.* **1995**, *9*, 1033.
2. (a) Michael, J. *Curr. Opin. Invest. Drugs.* **2003**, *4*, 1053; (b) Calkin, A. C.; Tontonoz, P. *Nat. Rev. Mol. Cell. Bio.* **2012**, *13*, 213; (c) Fievet, C.; Staels, B. *Biochem. Pharmacol.* **2009**, *77*, 1316; (d) Zhang, Y.; Chan, J.; Cummins, C. *Clin. Lipidol.* **2009**, *4*, 29–40; (e) Tontonoz, P.; Mangelsdorf, D. J. *Mol. Endocrinol.* **2003**, *17*, 985; (f) Lund, E. G.; Menke, J. G.; Spalow, C. P. *Arterioscler. Thromb. Vasc. Biol.* **2003**, *23*, 1169; (g) Calkin, A. C.; Tontonoz, P. *Arterioscler. Thromb. Vasc. Biol.* **2010**, *30*, 1513.
3. Terasaka, N.; Hiroshima, A.; Koieyama, T.; Ubukata, N.; Morikawa, Y.; Nakai, D.; Inaba, T. *FEBS Lett.* **2003**, *536*, 6.
4. Joseph, S. B.; McKilligin, E.; Pei, L.; Watson, M. A.; Collins, A. R.; Laffitte, B. A.; Chen, M.; Noh, G.; Goodman, J.; Hagger, G. N.; Tran, J.; Tippin, T. K.; Wang, X.; Lusis, A. J.; Hsueh, W. A.; Law, R. E.; Collins, J. L.; Willson, T. M.; Tontonoz, P. *Proc. Natl. Acad. Sci. U.S.A.* **2002**, *99*, 7604.
5. (a) Schultz, J. R.; Tu, H.; Luk, A.; Repa, J. J.; Medina, J. C.; Li, L.; Schwendner, S.; Wang, S.; Thoolen, M.; Mangelsdorf, D. J.; Lustig, K. D.; Shan, B. *Genes Dev.* **2000**, *14*, 2831; (b) Quinet, E. M.; Savio, D. A.; Halpern, A. R.; Chen, L.; Schuster, G. U.; Gustafsson, J.-Å.; Basso, M. D.; Nambi, P. *Mol. Pharmacol.* **2006**, *70*, 1340.
6. (a) Matsuda, T.; Okuda, A.; Watanabe, Y.; Miura, T.; Ozawa, H.; Tosaka, A.; Yamazaki, K.; Yamaguchi, Y.; Kurobuchi, S.; Koura, M.; Shibuya, K. *Bioorg. Med. Chem. Lett.* **2015**, *25*, 1274; (b) Preparation of compound **3**: Int. Patent Appl. WO2009107387, 2009.
7. (a) Svensson, S.; Ostberg, T.; Jacobsson, M.; Norstrom, C.; Stefansson, K.; Hallen, D.; Johansson, I. C.; Zachrisson, K.; Ogg, D.; Jendeberg, L. *EMBO J.* **2003**, *22*, 4625; (b) Hoerer, S.; Schmid, A.; Heckel, A.; Budzinski, R. M.; Nar, H. *J. Mol. Biol.* **2003**, *334*, 853; (c) Williams, S.; Bledsoe, R. K.; Collins, J. L.; Boggs, S.; Lambert, M. H.; Miller, A. B.; Moore, J.; McKee, D. D.; Moore, L.; Nichols, J.; Parks, D.; Watson, M.; Wisely, B.; Willson, T. M. *J. Biol. Chem.* **2003**, *278*, 27138; (d) Farnegardh, M.;

Bonn, T.; Sun, S.; Ljunggren, J.; Ahola, H.; Wilhelmsson, A.; Gustafsson, J. A.; Carlquist, M. *J. Biol. Chem.* **2003**, *278*, 38821.
8. Preparation of the type **5** compounds: Int. Patent Appl. WO2009122707, 2009.
9. Preparation of the type **6** and **7** compounds: Int. Patent Appl. WO2008065754, 2008.
10. Mitsunobu, O. *Synthesis* **1981**, 1.
11. (a) Friedel, P.; Crafts, J. M. *Compt. Rend.* **1877**, *84*, 1392; (b) Friedel, P.; Crafts, J. M. *Compt. Rend.* **1877**, *84*, 1450.
12. (a) Bergs, H. Ger. Pat. 566,094, **1929**; (b) Bucherer, H. T.; Fischbeck, H. T. *J. Prakt. Chem.* **1934**, *140*, 69; (c) Bucherer, H. T.; Steiner, W. T. *J. Prakt. Chem.* **1934**, *140*, 291; (d) Ware, E. *Chem. Rev.* **1950**, *46*, 403.
13. CHOK-1 cells with the LXRα/GAL4 or LXRβ/GAL4 hybrid and stably expressing the GAL4-responsive reporter vector pG5luc were seeded at a density of 20,000 cells/well on a 96-well plate in HAM-F12 medium containing 10% immobilized bovine fetal serum, 100 units/mL penicillin G, and 100 μg/mL streptomycin sulfate and incubated under a wet atmosphere with 5% CO_2 at 37 °C. After 24 h, medium with the test compound at various concentrations (0.01 μM, 0.1 μM, 1 μM, 10 μM, and 30 μM) was added, and the cells were incubated for an additional 24 h. The effect of the test compound on the activation of luciferase transcription via LXRα- or LXRβ-LBD was measured using Bright-Glo (Promega) as a luciferase assay substrate and measuring the luminescence intensity with an LB960luminometer (Berthold Technologies).
14. (a) The acidic hydroxyl oxygen atom of 1,1-bistrifluoromethyl-carbinol is located in a favorable position for donating a proton to the Nε imidazole nitrogen of His435 and results in a strong hydrogen-bonding interaction. Bennett, D. J.; Carswell, E. L.; Cooke, A. J.; Edwards, A. S.; Nimz, O. *Curr. Med. Chem.* **2008**, *15*, 195; (b) The Amgen group reported that blocking the hydroxyl group significantly reduced the potency in a series of T0901317 derivatives, which indicates that the 1,1-bistrifluoro-methylcarbinol moiety plays an important role in LXRα activation. These reports prompted us to design the disconnection of the C–O–C bond of 1,3-dihydroisobenzofuran. Li, L.; Liu, J.; Zhu, L.; Cutler, S.; Hasegawa, H.; Shan, B.; Medina, J. C. *Bioorg. Med. Chem. Lett.* **2006**, *16*, 1638.
15. Srivastava reported that the hyperlipidemic Bio F_1B hamster has been proven to be an adequate atherosclerosis model for the evaluation of lipid-modulating agents. Srivastava, R. A. K. *Atherosclerosis* **2011**, *214*, 86–93. However, the above experimental condition requires 21 weeks for the evaluation. To reduce the experimental period to 10 weeks, we conducted our established protocol as described in the following Letter: Ikenoy, M.; Yoshinaka, Y.; Kobayashi, H.; Kawamine, K.; Shibuya, K.; Sato, F.; Sawanobori, K.; Watanabe, T.; Miyazaki, A. *Atherosclerosis* **2007**, *191*, 290.
16. Interestingly, Srivastava reported that T0901317 does not alter the LDL-C level but results in a three-fold increase in the TG level and a 50% increase in the HDL-C level under the fed condition. Our pharmacological experimental details are described in the Supplementary data.
17. A solution of **62** in PEG400 was orally administered to a hamster fed the CE-2 chow diet. Blood samples (heparin plasma) were collected from a forearm vein 0.5, 1, 2, 3, 4, 6, 8, 10 and 24 h after administration. The drug concentrations of **62** and **70** in the supernatant were measured by HPLC-MS/MS. Our pharmacokinetic experimental details are described in the Supplementary data.
18. In an in vivo study with a Bio F_1B hamster, we measured the gene expression of ABCA1 in the intestine and peripheral blood as shown in the Table. ABCA1 in the intestine was upregulated in a dose-dependent manner, but ABCG5 and ABCG8 were not significantly altered. Increased intestinal ABCA1 expression contributes to the decrease in cholesterol absorption. See the reference. Plat, J.; Mensink, R. P. *FASEB J.* **2002**, *16*, 1248–1253. Similarly, ABCA1 in the peripheral blood was not sufficiently upregulated to contribute to the increases in HDL-C and RCT. These results led us to draw the previously mentioned conclusion.

Compound	Dose (mg/kg)	ABCA1 intestine (fold)	ABCA1 peripheral blood (fold)	ABCG5 intestine (fold)	ABCG8 intestine (fold)
T0901317	10	3.4*	1.3	1.5	1.4
62	10	2.1*	1.0	1.2	1.3
	30	4.0*	0.8	1.5	1.4
	100	5.2*	1.0	1.3	1.3

*$p<0.05$; the statistical analysis was conducted using Dunnett's test.
The fold value was calculated relative to the control.